Phase Transitions Involving Molecular Reorientation in a Series of Copoly(ester imide)s

Mark Leland, Zongquan Wu, Rong-Ming Ho, and Stephen Z. D. Cheng*

The Maurice Morton Institute and Department of Polymer Science, University of Akron, Akron, Ohio 44325-3909

Hans R. Kricheldorf

Institut für Technische und Makromolekulare Chemie, Universität Hamburg Bundesstrass 45, D-20146 Hamburg 13, Federal Republic of Germany

Received August 5, 1997; Revised Manuscript Received October 31, 1997[⊗]

ABSTRACT: A series of copoly(ester imide)s (CPEIs) was synthesized by the esterification of *N*,*N*′-dodecane-1,12-diylbis(trimellitimide) to two different acetylated diols, 4,4′-dihydroxybiphenyl and hydroquinone, in varying proportions. Six samples were prepared and are designated as CPEI(A−F). CPEI(A) is a homopolymer having 100% of incorporated 4,4′-dihydroxybiphenyl and CPEI(F) is a homopolymer having 100% of incorporated hydroquinone. The composition ratios of the copolymers are 80/20 (B), 60/40 (C), 40/60 (D), and 20/80 (E). With the exception of CPEI(F), the copolymers show enantiotropic smectic C phases. All of the samples exhibit highly ordered crystalline phases in the solid state. The nature of these phases has been found to depend on the thermal history of the samples with the existence of two possible molecular orientations with respect to the smectic layers. The first arrangement involves an alignment of the molecules parallel to the layer normal while the second arrangement involves tilted molecular alignment. Both appear to possess the same lateral packing dimensions and symmetry within the layers which is rectangular in the plane perpendicular to the chain direction. The three-dimensional lattice is thus orthorhombic in the case of the parallel molecular alignment and monoclinic ($\beta \neq 90°$) in the case of the tilted molecular alignment. Of the two arrangements the orthorhombic one appears to be more stable than the monoclinic one. Therefore, the phase associated with the monoclinic arrangement is accessible through a monotropic transition. A transition between these two arrangements occurs *via* structural melting and new order development upon heating. The presence of these two arrangements provides a unique opportunity to assess the origin of the anomalous orientation found in this series of copolymers.

Introduction

Although aromatic polyimides possess relatively rigid chain backbones, it is difficult to find reports on the existence of thermotropic liquid crystalline states.[1] Recently, one incidence of thermotropic liquid crystals has been found in polyimides with different numbers of methylene units.[2,3] In the case of modified polyimides, such as poly(ester imide)s, liquid crystalline behavior is more commonly observed.[1,4−8] In one of our research laboratories (University of Hamburg, Germany), a series of copoly(ester imide)s (CPEIs) has been synthesized from the esterification of *N*,*N*′-dodecane-1,12-diylbis(trimellitimide) to two different acetylated diols, 4,4′-dihydroxybiphenyl and hydroquinone, in varying proportions.[9,10] On the basis of variations of the composition, six samples were prepared and are designated as CPEI(A−F) in which CPEI(A) is a homopolymer having 100% of the 4,4′-dihydroxybiphenyl-based ester group and CPEI(F) is a homopolymer having 100% of the hydroquinone-based ester group. Following the alphabetic sequence, the composition ratios of the copolymers are 80/20 (B), 60/40 (C), 40/60 (D), and 20/80 (E) of the 4,4′-dihydroxybiphenyl and hydroquinone groups, respectively.

Initial results demonstrated that CPEI(A) shows liquid crystalline behavior as well as anomalous fiber orientation in which the molecules appear to be oriented perpendicular to the fiber direction.[10] Later, wide-angle X-ray diffraction (WAXD) fiber experiments provided further evidence of this anomalous orientation in CPEI-(A−E). The nature of this observation has been explained in detail on the basis of crystallographic knowledge.[11] This unusual phenomenon has been reported in the literature for a few other liquid crystalline materials in both melt-spun fibers as well as sheared samples.[12−15] Our previous report attributed this behavior to the alignment of smectic layers instead of individual molecules similar to the formation mechanism originally proposed.[13,14]

Previous work in our laboratory has focused on the identification of highly ordered smectic and smectic crystal phases in a series of polyethers.[16−18] It has been demonstrated that there is a direct correspondence between these phases found in polymeric samples with those initially established for small molecule liquid crystals.[19−21] In this publication, we will report that CPEI(A−E) show a low-ordered liquid crystalline smectic C (S_C) phase at high temperatures. Moreover, this series of CPEIs possesses a monotropic, highly ordered smectic crystal phase with a monoclinic (M) unit cell in addition to a more stable phase with an orthorhombic (O) unit cell. Both phases have the same lateral packing dimensions and symmetry when viewed parallel to the molecular chain direction. The apparent differences between these two phases involve their molecular orientation with respect to the layer normal and the

* To whom correspondence should be addressed.

[⊗] Abstract published in *Advance ACS Abstracts,* December 15, 1997.

S0024-9297(97)01198-4 CCC: $15.00
Published on Web 01/13/1998

Table 1. CPEI Materials

name	% biphenyl/% hydroquinone	η_{inh} (dL/g)[a]
A	100/0	N/A
B	80/20	0.94
C	60/40	0.48
D	40/60	0.58
E	20/80	0.40
F	0/100	0.34

[a] Inherent viscosity determined in a 2 g/L solution in trifluoroacetic acid/methylene chloride (1:4).

lateral order correlation. The presence of these two phases also permits a unique opportunity to further examine the origin of the anomalous orientation in this series of materials.

Experimental Section

Materials and Samples. The series of CPEIs was prepared by the esterification of *N*,*N*′-dodecane-1,12-diylbis(trimellitimide) to two different acetylated diols, hydroquinone and 4,4′-dihydroxybiphenyl, in varying proportions. The chemical structure of this series of CPEIs is shown below:

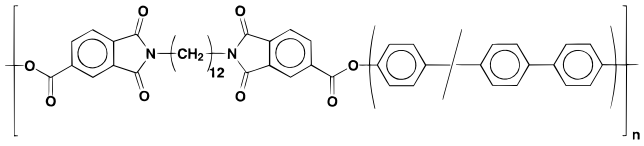

Table 1 shows the abbreviations for the system used in this publication as well as the proportions of the two ester groups and the inherent viscosities of the polymers taken from a 2 g/L solution of the polymer in dichloromethane/triflouroacetic acid (4:1) at 20 °C. Note that for the material containing only the biphenyl moiety, CPEI(A), the inherent viscosity is not available due to the insolubility of this material.

Fibers of each CPEI sample were prepared by drawing from the liquid crystalline phase when applicable. Due to the limited tensile strength of the fibers, no further drawing was imposed on them, although the fibers were annealed at elevated temperatures below the solid-to-liquid crystal transition temperatures. The thin films prepared for transmission electron microscopy (TEM) were solution cast with a thickness of 100−300 nm. The film samples were also mechanically sheared at temperatures slightly lower than the isotropization temperatures observed in differential scanning calorimety (DSC).

Equipment and Experiments. DSC was performed on a Perkin-Elmer DSC-7 with a cooling apparatus. The temperature and heat flow were calibrated using standard materials at different cooling rates between 2.5 and 40 °C/min.

Reflection WAXD experiments were conducted with a Rigaku 12 kW rotating-anode generator (Cu Kα) coupled with a Geigerflex D/max-RB diffractometer. The X-ray beam was line-focused and monochromatized using a graphite crystal. The reflection peak positions and widths were carefully calibrated with silicon crystals of known crystal size in the high-angle region ($>2\theta = 15°$) and silver behenate in the low-angle region ($<2\theta = 15°$). For WAXD powder patterns taken at room temperature, a scanning rate of 0.5°/min was used in the 2θ angle region of 1.5°−35°. The heating and cooling experiments at 2 °C/min were also performed using WAXD with a hot stage. The scanning rate in this case was 7°/min in the selected 2θ angle range. Background scattering was carefully recorded and subtracted from the WAXD patterns. Fiber WAXD patterns were obtained using a flat-plate vacuum camera attached to a Rigaku tube X-ray generator. Exposure times ranged from 1 to 5 days in order to identify both strong and weak reflections. The same calibration procedure described previously was followed. Fiber patterns were also collected using the rotating anode in conjunction with a Siemens area detector in order to perform azimuthal integration. The unit cell determination procedure based on the reciprocal lattice approach was described in detail in one of our early publications.[22] Computer refinement was conducted to achieve the fit with the least error between experimental results and calculated data on the basis of a continuous refinement program established in our laboratory.[22]

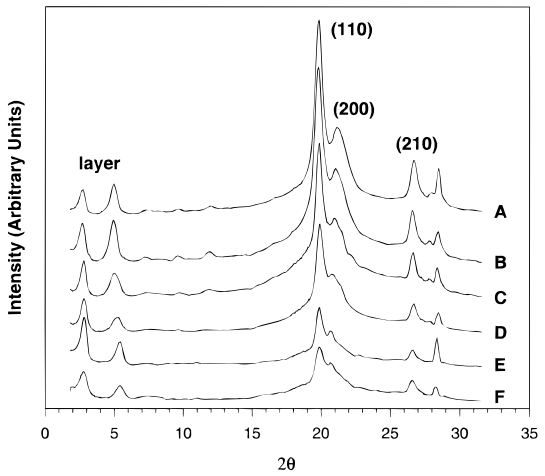

Figure 1. WAXD powder patterns for CPEI(A−F) after the samples were crystallized at high temperatures and slowly cooled to room temperature.

A TEM of JEOL (1200 EX II) was utilized to confirm the morphologies observed in the samples. An accelerating voltage of 120 kV was used. The thin films were shadowed with Pt and coated with carbon for TEM observations. For electron diffraction (ED) experiments, spacing calibration was done using TlCl in a *d*-spacing range smaller than 0.384 nm, which is the largest spacing for TlCl. Spacing values larger than 0.384 nm were calibrated by doubling the *d*-spacing of those reflections based on their first-order reflections.

Results and Discussion

Identification of Phase Structures. The WAXD powder patterns for CPEI(A−F) are shown in Figure 1. Each sample was annealed for several hours at temperatures just below the temperature at which the liquid crystal phase is assumed and slowly cooled to room temperature prior to the measurement. An initial review of Figure 1 suggests a great deal of similarity in all of the samples. There are at least two reflections at low angles ($2\theta < 10°$) which should correspond to the first- and second-order reflections of a layer spacing in the ordered structure (as demonstrated by WAXD fiber patterns and ED experiments, see below). At higher angles ($2\theta > 10°$) there are three distinct reflections which should be associated with lateral packing order within the layers. In order to prove this expectation, single crystals of the CPEI(B−F) were grown at elevated temperatures. One such crystal of CPEI(F) is shown in Figure 2 with its corresponding ED pattern. The [00*l*] zone diffraction indicates two-chain rectangular lateral packing of the samples with one chain at the center and four one-fourth chains at the corners. The zone axis is parallel to the chain (*c*-) axis. Comparison of the *d*-spacing from both ED and WAXD powder patterns shows good agreement among the data and permits the 110, 200, and 210 reflection assignments shown in Figure 1. This indicates that the high-angle reflections in Figure 1 indeed represent the lateral order in the structures.

After high-temperature annealing, CPEI(A−F) exhibit an arrangement of the molecules parallel to the layer normal. Indirect evidence of this arrangement is

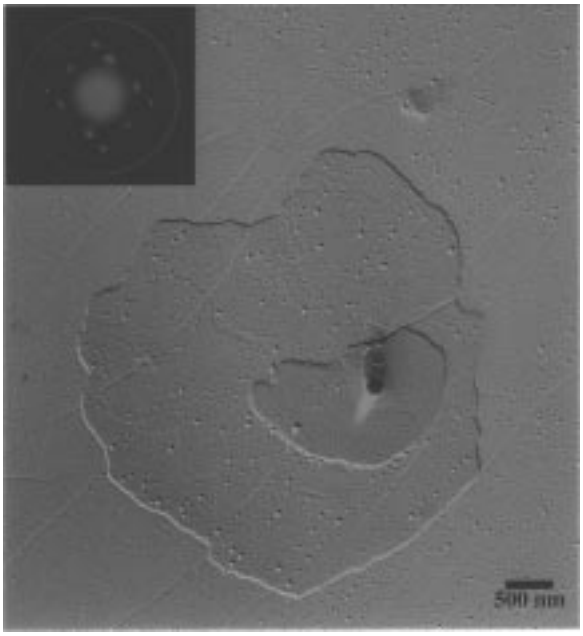

Figure 2. TEM photograph of a single crystal of CPEI(F) and corresponding [00*l*] zone ED pattern.

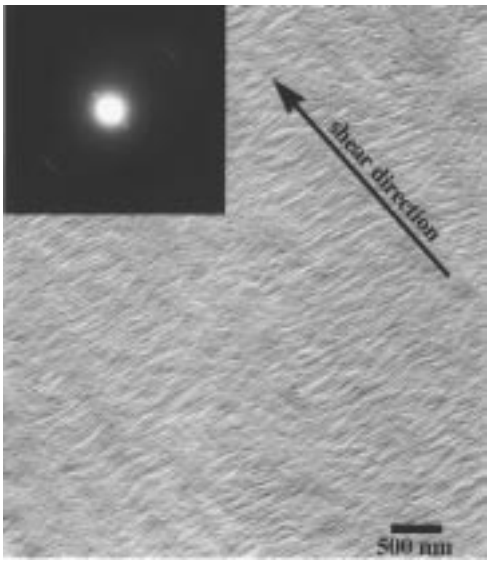

Figure 3. TEM photograph of a sheared CPEI(E) sample after annealing and the corresponding ED pattern.

afforded by the [00*l*] zone ED in Figure 2 achieved without the necessity of sample tilting. More direct evidence is provided by the ED of sheared samples after annealing such as that shown for CPEI(E) in Figure 3. In this figure, the micrograph reveals a perpendicular arrangement of lamellar stacks (with the lamellar thickness ranging from 30 to 40 nm) with respect to the shear direction. From the insert ED in Figure 3, the molecules are arranged parallel to the lamellar normal and therefore, parallel to the shear direction. This arrangement coupled with the rectangular lateral packing of the molecules within the layers indicates that the samples possess an orthorhombic (O) unit cell.

The unit cell parameters were calculated for each sample and are listed in Table 2. The layer dimensions are based on WAXD data, while the lateral *a*- and *b*-dimensions are obtained from both WAXD and ED results. Proceeding from CPEI(A) to CPEI(F), associated with a decrease in the content of incorporated

Table 2. Ordered Structure Dimensions in CPEIs

dimension	A	B	C	D	E	F
a (nm)[a]	0.863	0.868	0.869	0.869	0.869	0.871
b (nm)[a]	0.526	0.525	0.524	0.523	0.521	0.518
layer (nm)	3.72	3.68	3.68	3.54	3.33	3.33
ρ (g/cm^3)[a]	1.37	1.35	1.32	1.35	1.40	1.38
tilt angle	32°	31°	31°	27°	22°	22°

[a] Based on a two-chain orthorhombic packing.

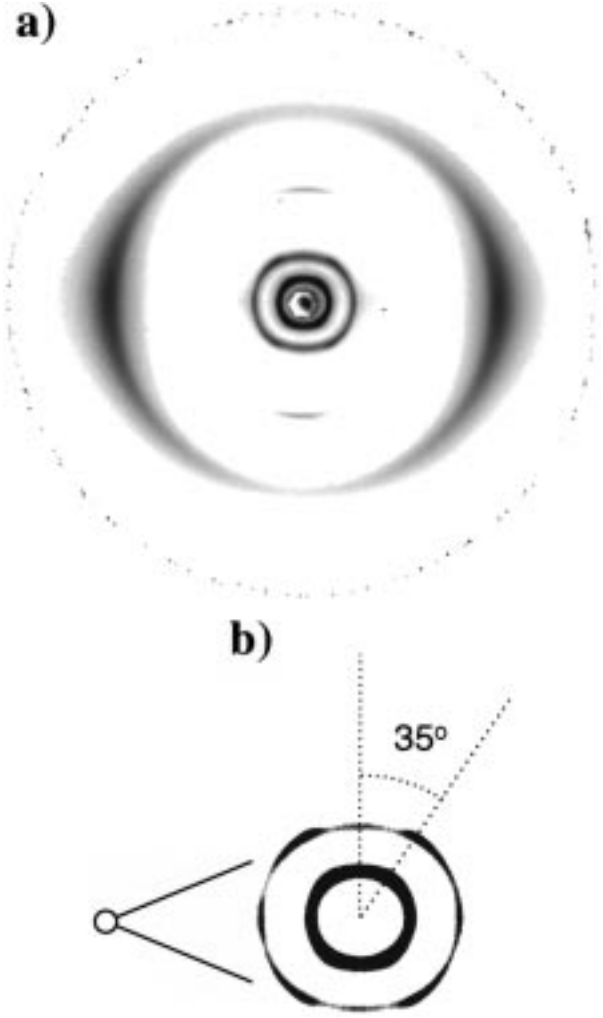

Figure 4. WAXD fiber patterns for (a) CPEI(B) and (b) an enlarged low-angle region of Figure 4a. Fiber direction is vertical on the page.

biphenyl, there is a slight increase in the *a*-dimension and a slight decrease in the *b*-dimension. The magnitude of these changes are small, suggesting that the nature of the ester groups has only a minimal effect on the lateral molecular packing within the layers. The proximity of the values suggests the possibility of cocrystallization of the two types of ester groups. From Table 2, it is clear that there is an increase in the layer spacing as the percent of incorporated biphenyl increases as would be expected due to the greater length of this diol. The presence of a single layer spacing also implies cocrystalliztion of the two types of incorporated esters.

Evidence exists for the presence of a second arrangement involving a tilt of the molecules with respect to the layer normal. One example is shown in Figure 4a for CPEI(B) quenched from high temperatures after fiber spinning. In the WAXD fiber pattern, the mol-

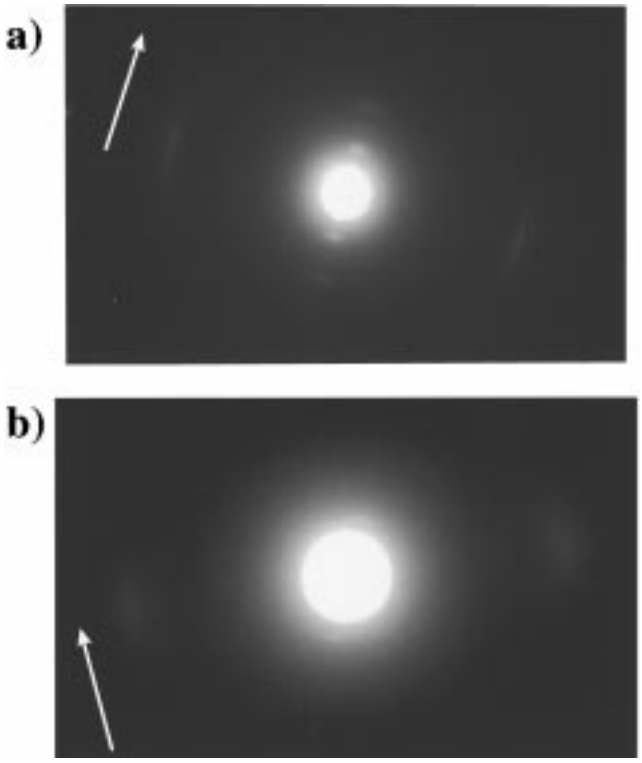

Figure 5. ED patterns for CPEI(B) (a) with the parallel molecular alignment (sample was annealed at 278 °C) and (b) with the tilted molecular alignment (sample was fast-cooled to room temperature). Arrows indicate directions of shear.

ecules appear to be predominantly aligned parallel to the fiber direction as indicated by the presence of the 110 and 200 reflections on the equator. However, the position of the layer reflections is less straightforward. The first- and second-order reflections are enlarged in Figure 4b. This figure shows intensification of the layer reflections in quadrant, indicating a tilted layer normal with respect to the molecular alignment (along the fiber meridian direction) as well as some intensification of the reflections on both the equator and the meridian. The presence of the layer reflections on the equator is indicative of the anomalous orientation discussed in a previous publication.[11] Note that a strong fifth-order refection is also visible on the meridian for this arrangement. At this moment, we do not know the cause of this reflection. It may be associated with chain orientation and packing. The appearance of the layer reflections on the meridian indicates the presence of the O arrangement discussed previously. For the reflections appearing in quadrant, the intensity profile along the azimuthal angle of the second-order layer reflection reveals a tilt angle of ±35° between the molecular chain direction and layer normal.

Further evidence for both types of arrangements can be found in ED of sheared samples. Shown in Figures 5a and 5b are the ED patterns from two samples of CPEI(B). In Figure 5a, the parallel alignment of the molecules with respect to the layer normal is found after the sample was sheared and annealed at a temperature of 278 °C. On the other hand, the sample in Figure 5b was quickly cooled to room temperature after being sheared. On the basis of an evaluation of the intensity maxima for both the (*hk*0) on the equator and layer reflection in the quadrant in Figure 5b, the tilt angle between the molecules and the layer normal is geometrically estimated to be 30°.

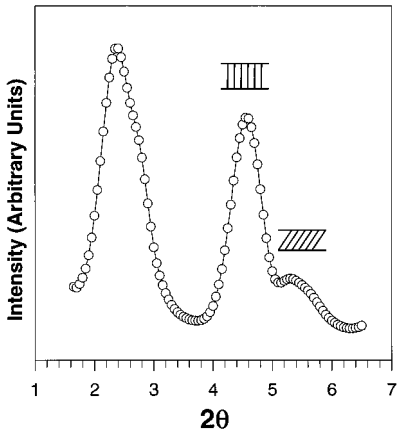

Figure 6. WAXD powder pattern in the low-angle region for CPEI(B) cooled to room temperature at a rate of 2 °C/min.

The presence of both arrangements is also detectable in the WAXD powder patterns as can be seen in the doublet of the layer reflection in Figure 6 for CPEI(B) (the doublet of the second-order layer reflections is more prominent due to a better separation at higher 2θ angles compared with the first-order reflections at lower 2θ angles). The sample in Figure 6 was cooled to room temperature from the isotropic melt at a cooling rate of 2 °C/min. The tilted molecular alignment results in a smaller layer spacing and hence, appears at higher 2θ angles than the parallel alignment. On the basis of a simple geometric ratio of the two layer spacings, an estimate of the tilt angle can be calculated. For Figure 6 this value is found to be 32°. Therefore, the similarity in the tilt angle values found in the three different experimental observations discussed above is evident within an expected level of experimental error.

The tilt angle for each polymer calculated from the WAXD and ED results is also included in Table 2. Note that this set of data is attributed to the tilted molecular alignment and is unrelated to the O unit cell. The tilt angles for CPEI(A−C) are similar within the range of experimental error (±2°). CPEI(D) shows a slight decrease in its tilt angle and CPEI(E, F) exhibit lower tilt angles. It should be noted that the overlapped reflection peaks for CPEI(E, F) make the evaluation of tilt difficult. In the case of these two materials, the necessity of peak separation leads to a larger degree of experimental error (±5°). This arrangement signifies a monoclinic (M) unit cell due to the tilted molecular chain direction with respect to the layer normal. Within the layers there appears to be little difference in the lateral packing dimensions and symmetry between both the O and M arrangements. DSC experiments reveal that the degree of undercooling for this transition is similar to that found in the formation of the S_C phase (see below), suggesting that this phase structure is truly a smectic crystal as opposed to a crystal phase. Furthermore, the M arrangement indicates that this phase is either a smectic crystal H or K phase.[11,16−21]

Classification of the phase with the O arrangement requires further discussion. Although the similarity in lateral packing dimensions and symmetry of this phase to the phase of the M arrangement, the development of the O arrangement seems to be dependent upon the cooling rate (as discussed below), which is usually not the case for highly ordered smectic crystal phases.[16−18] Moreover, the order correlation associated with the lateral packing of 200, 110, and 210 reflections in this

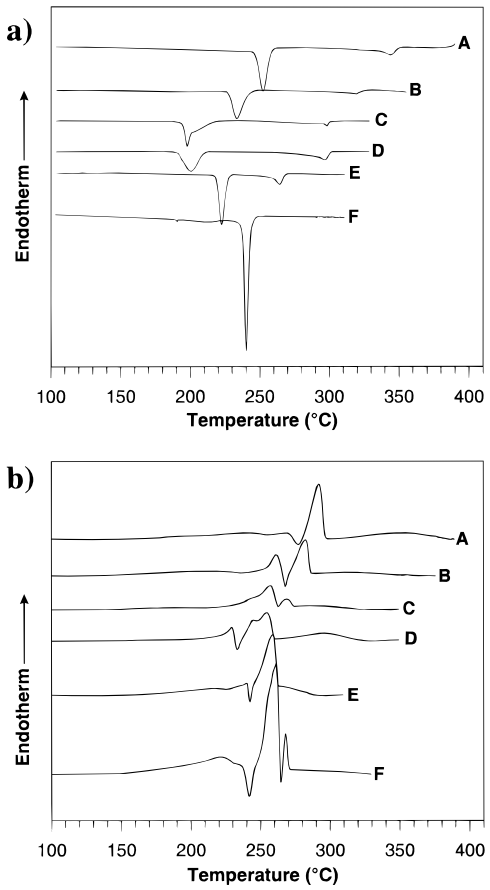

Figure 7. DSC curves for CPEI(A−F) (a) at a cooling rate of 10 °C/min and (b) at a heating rate of 10 °C/min.

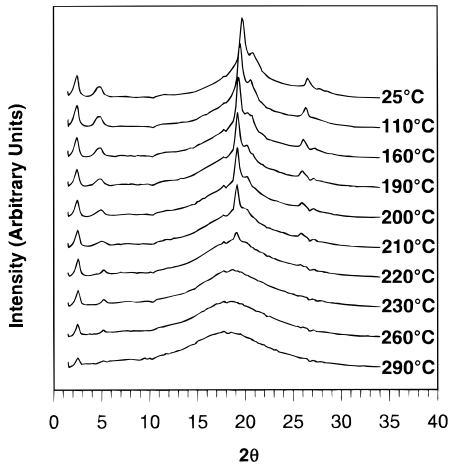

Figure 8. WAXD powder patterns for CPEI(D) during cooling at a cooling rate of 2 °C/min.

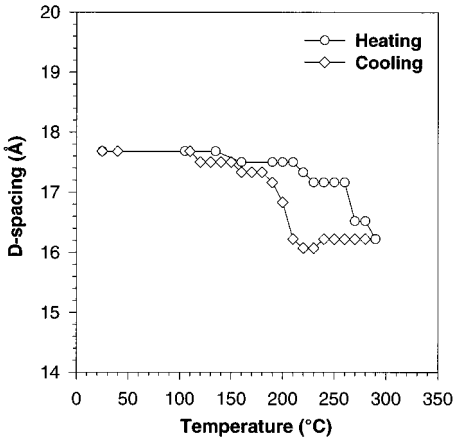

Figure 9. The *d*-spacing of the second-order layer reflection of CPEI(D) during heating and cooling at 2 °C/min.

phase is significantly higher than that for the phase with the M arrangement. This leads to a qualitative conclusion that the phase having the O arrangement may be more ordered than that with the M arrangement.

The origin of the cooling rate dependence can be investigated *via* observing thermal transitions of CPEI-(A−F) as shown in Figure 7. From the cooling curves (Figure 7a), it is clear that CPEI(A−E) exhibit two transitions upon cooling, while CPEI(F) exhibits only a single transition which corresponds to the lower temperature transition in the other CPEIs. The higher temperature transitions in CPEI(A−E) show a minimal degree of undercooling, indicative of the formation of a liquid crystalline phase. On the basis of WAXD powder results, this transition in CPEI(A−E) has been identified with the onset of layer order in the absence of lateral packing order within the layers. This is an indication of a smectic liquid crystalline A (S_A) or C (S_C) phase. The lower temperature transition, present in CPEI(A−F), is associated with the development of lateral packing order within the layers as shown in Figure 8 for CPEI(D).

In order to determine whether the low-ordered smectic phase is a S_A or S_C phase, it is necessary to carefully examine the layer spacing during the transition. Shown in Figure 9 is a plot of the layer spacing of the second-order reflection for CPEI(D) *versus* temperature during both heating and cooling at 2 °C/min. On the basis of the *d*-spacing of the layer reflection, the sample begins in the phase with the O arrangement. When the sample is heated above the second endotherm in the DSC heating diagram, the lateral packing order is lost, indicating the transformation into the low-ordered smectic phase. At the same time, a shift is found in the layer spacing which correlates to the M arrangement. Thus, this low-ordered smectic phase is a S_C phase.

The presence of the S_C phase indicates that the development of the phase with the O arrangement requires a cooperative molecular reorientation from a tilted molecular alignment in the S_C phase to a parallel molecular alignment with respect to the layer normal. Hence, the greater undercooling dependence found for this phase is understandable due to a greater kinetic barrier caused by this reorientation. By the samples being cooled at increasingly slow rates, the percentage of the phase with the O arrangement increases at the expense of the less stable phase with the M arrangement as shown in Figure 10 for CPEI(D).

Phase Transition Behavior. From the DSC heating curves in Figure 7b, it can be seen that all of the CPEIs show complex melting behavior during heating. At the highest temperatures CPEI(A−E) exhibit a broad transition which corresponds to the transition from the S_C phase to the isotropic melt. This transition is conspicuously absent in CPEI(F) and indicative of the fact that this material does not exhibit the S_C phase but transfers directly from the highly ordered phase into the isotropic melt. Prior to the onset of the S_C phase [or isotropic melt in the case of CPEI(F)] all of the copolymers undergo structural melting (endother-

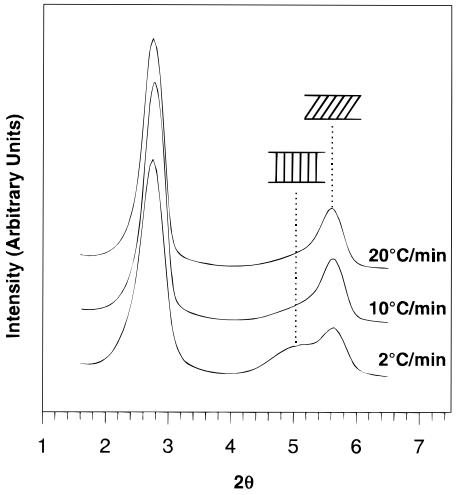

Figure 10. WAXD powder patterns in the low-angle region for CPEI(D) at different cooling rates to generate two different molecular alignments.

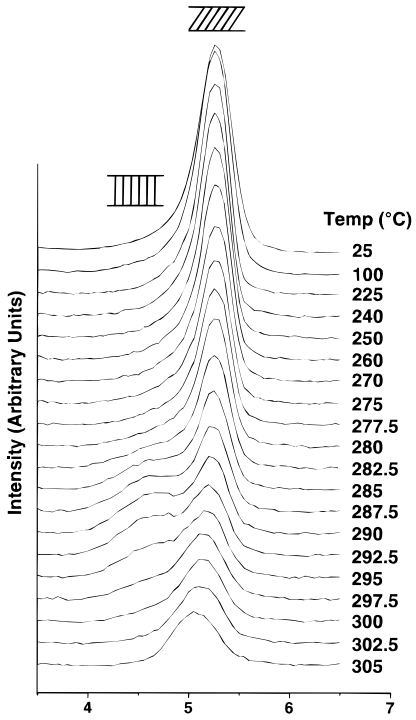

Figure 11. WAXD powder patterns of the second-order layer reflection of CPEI(B) during heating.

mic), new order development (exothermic), and structural remelting (endothermic) processes to varying extents. These three thermal events appear to be overlapped.

The three thermal events observed in DSC (Figure 7b) can be explained using the results of WAXD powder patterns during heating. Figure 11 shows the second-order layer reflection of CPEI(B) taken during heating. The sample has been prepared by fast cooling from the isotropic melt to room temperature to maximize the presence of the M arrangement. Initially, the material exhibits a layer spacing at higher 2θ angles associated with this arrangement. Upon heating to the lowest endothermic peak (260 °C), a clear decrease can be found in the layer reflection intensity (a 23% drop between 240 and 280 °C). This indicates that as the sample is heated, the highly ordered smectic crystal phase with the M arrangement melts into the S_C phase.

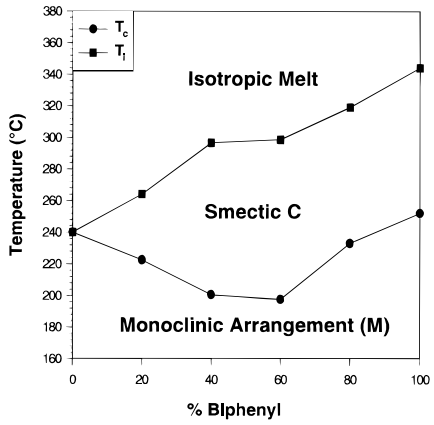

Figure 12. Transition temperatures obtained through extrapolation to a 0 °C/min cooling rate for CPEI(A−F) with respect to the biphenyl ester contents.

Since the S_C phase also possesses the same tilted molecular alignment, this layer reflection does not completely disappear. Further heating elicits the development of a second layer reflection at lower 2θ angles associated with the O arrangement. This phase development corresponds to the exothermic (new order development) process observed in DSC at around 270 °C for CPEI(B). The subsequent remelting process in the DSC is marked by the disappearance of the low-angle layer reflection corresponding to the O arrangement. Only the tilted layer reflection is retained, consistent with the existence of the S_C phase up to the isotropization temperature. During these structural transformations, the lateral packing dimensions and symmetry do not seem to change prior to the final melting endotherm. The only apparent changes in the d-spacings of the lateral packing reflections (110, 200, and 210) correspond to thermal expansion.

The phase transition behavior for CPEI(A−F) is shown in Figure 12 based on DSC cooling experiments. The transition temperatures were obtained by extrapolating the data at different cooling rates to a 0 °C/min cooling rate. The onset temperature of the S_C phase decreases as the amount of incorporated biphenyl decreases down to CPEI(F) which does not exhibit the S_C phase. This reveals that the biphenyl unit stabilizes the liquid crystal phase by imparting either sufficient rigidity and/or regularity to the samples. Furthermore, the absence of the S_C phase in CPEI(F) suggests that the presence of the biphenyl unit is necessary for this series of samples to exhibit this phase. Faster cooling rate data was used in the determination of the lower temperature transition. Thus, the boundary plotted is representative of the phase with the M arrangement. It should be noted that the samples may assume the O arrangement when the cooling rate is sufficiently slow. Another set of extrapolations may thus generate the boundary of this phase. In theory, the equilibrium transition temperatures of this boundary should be higher than those of the phase with the M arrangement. Clearly, as the comonomer composition approaches 50%, the onset temperatures of lateral structural formation exhibit a minimum as might be expected due to the greater irregularity present in such samples.

On the basis of the analyses of WAXD and DSC results, the relative thermodynamic stabilities of the phases with the O and M arrangements can be under-

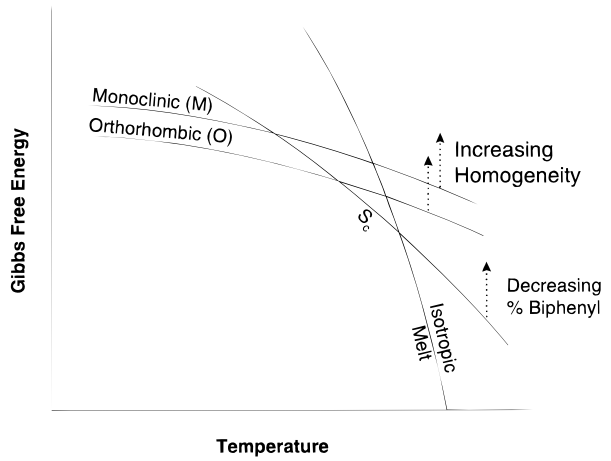

Figure 13. Schematic plot between Gibbs free energy and temperature at constant pressure to illustrate different phase transition behavior.

Figure 14. WAXD fiber pattern for CPEI(A) with anomalous orientation behavior. Fiber direction is vertical on the page.

stood. Clearly, the transition from the M to O arrangement upon heating indicates the higher stability of the latter. In addition, as seen in Figure 10, rapid cooling favors the formation of the phase with the M arrangement. Due to the cooperative molecular reorientation necessary for the formation of the O arrangement from the S_C phase, the molecules may assume the M arrangement, although it is thermodynamically less stable, because it is kinetically more accessible. Consequently, upon subsequent slow heating the CPEIs return to the more stable O arrangement if sufficient molecular mobility is provided. Therefore, by definition the phase with the M arrangement is phenomenologically monotropic with respect to the O arrangement.

The transition temperature and thermodynamic stability in the respective phases can be described in a plot of the Gibbs free energy *versus* temperature at constant pressure as shown in Figure 13. In the case of CPEI-(F), the S_C line may be pushed toward high values of the Gibbs free energy. Therefore, this phase cannot be experimentally observed. The less stable phase with the M arrangement is only accessible by rapid cooling capable of providing sufficient undercooling to reveal the monotropic transition. In the case that a sample assumes this phase, during heating the sample will melt at the intersection of this line with the S_C line entering the low-ordered smectic phase through a first-order transition. In the S_C phase, the molecules gain sufficient mobility to assume the more stable O arrangement. Further heating elicits melting of this phase into the S_C phase and finally the isotropic melt for CPEI-(A−E). Slower cooling allows direct formation of the phase with the O arrangement which melts directly into the S_C phase upon subsequent heating. Introduction of comonomers in the samples causes a destabilization of both the O and M phases, causing these lines to shift to higher energy levels and creating lower transition temperatures. An increase in the incorporated biphenyl increases the stability (i.e., lowers the free energy) of the S_C phase. This leads to the increase in the transition temperatures seen upon cooling for copolymers with greater amounts of incorporated biphenyl.

It is worthy to note that the phase transitions in this series of samples represents an unusual situation. The similarity in lateral packing dimensions and symmetry between the phases with the O and M arrangements alone is quite remarkable, while the interchange between these two arrangements is somewhat unexpected. A similar observation of the existence of a transformation from a S_C to a S_A phase between the crystal melting and isotropization temperatures in a copoly(ester imide) was also recently reported.[23]

Anomalous Molecular Orientation. As has been documented in a previous publication, this series of CPEIs has the tendency to assume an orientation in which the molecules appear to be aligned perpendicular to the axis of draw.[11] The ramifications of this type of orientation have already been discussed in regard to a parallel alignment of the molecules with respect to the layer normal. In the case of molecules which are tilted with respect to the layer normal, a similar analysis can be expected. In this instance, the reflections associated with the lateral packing order within the layer (e.g., 110 and 200) are expected to be diffused along the azimuthal angle regardless of the degree of orientation found in the layer-spacing reflections. In addition, the intensity is expected to decay to some non-zero value near the equator of the fiber diffraction pattern. However, in this case the maximum intensity is expected to appear in the quadrant at some angle associated with the angle of inclination between the molecules and the layer normal. Actual experimental observations of these reflections may be spread more along the azimuthal angle than predicted due to the less than perfect orientations of the smectic layers.

A fiber pattern of CPEI(A) is shown in Figure 14. The presence of the layer reflections on the equator indicates that the fiber possesses anomalous orientation. In addition, there is a doublet of the second-order layer reflection which indicates that the sample possesses both the O and M arrangements. If the origin of anomalous orientation in this series of CPEIs was dictated by preferred orientation of the molecules perpendicular to the direction of flow, the layer reflection associated with the tilted molecular alignment would be expected to appear in quadrant. Hence, the presence of this reflection on the equator is a strong indication that the origin of the anomalous orientation is associated with the orientation of the smectic layers and/or domains comprised of several smectic layers. Thus, in this series of samples the anomalous orientation does not appear to

arise from an intrinsic tendency of the individual molecules to orient perpendicular to the fiber draw direction. Two supplemental points also suggest that the anomalous orientation arises from the orientation of the layer structures. First, fibers were drawn from the S_C phase, and second, the anomalous orientation is only found in CPEI(A−E) which possess the S_C phase and not in CPEI(F) which does not.

Conclusion

CPEI(A−F) assume two arrangements which are only distinguished by the molecular orientation with respect to the layer normal. In their most stable form, the copolymers exhibit an O arrangement. However, another solid-state phase exists which involves the same lateral packing dimension and symmetry when viewed along the molecular axis but a tilted molecular alignment with respect to the layer normal (a M arrangement). The M arrangement is accessible by rapid cooling due to a limited undercooling dependence of the transition temperatures, and it may be viewed as a highly ordered smectic crystal phase. The more stable phase with the O arrangement is accessible by either slower cooling or subsequent slow heating from the phase with the M arrangement. This illustrates that the M arrangement is monotropic with respect to the phase with the O arrangement. CPEI(A−E) exhibit a S_C phase prior to isotropization upon heating while CPEI(F) melts directly into the isotropic melt. It appears that the biphenyl comonomer unit acts to stabilize the liquid crystal phases. The presence of the two possible arrangements provides a unique opportunity to investigate the origin of the anomalous orientation. The results suggest that for this series of CPEIs the anomalous orientation arises from orientation of the smectic layers and/or domains comprised of several smectic layers.

Acknowledgment. This work was supported by the Division of Materials Research, National Science Foundation (DMR-9157738 and DMR-9617030).

References and Notes

(1) Kricheldorf, H. R. *Mol. Cryst. Liq. Cryst.* **1994**, *254*, 87.
(2) Inoue, T.; Kakimoto, M.; Imai, Y.; Watanabe, J. *Macromol. Chem. Phys.* **1997**, *198*, 519.
(3) Kaneko, T. I.; Imamura, K.; Watanabe, J. *Macromolecules* **1997**, *30*, 4244.
(4) Kricheldorf, H. R.; Pakull, R. *Eur. Polym.* **1987**, *28*, 1772.
(5) Kricheldorf, H. R.; Pakull, R. *Macromolecules* **1988**, *21*, 551.
(6) Pardey, R.; Harris, F. W.; Cheng, S. Z. D.; Aducci, J.; Facinelli, J. V.; Lenz, R. W. *Macromolecules* **1992**, *25*, 5060.
(7) Pardey, R.; Harris, F. W.; Cheng, S. Z. D.; Aducci, J.; Facinelli, J. V.; Lenz, R. W. *Macromolecules* **1993**, *26*, 3687.
(8) Pardey, R.; Pardey, R.; Wu, S. W.; Chen, J.-H.; Harris, F. W.; Cheng, S. Z. D.; Keller, A.; Aducci, J.; Facinelli, J. V.; Lenz, R. W. *Macromolecules* **1994**, *27*, 5794.
(9) Kricheldorf, H. R.; Pakull. R. *Polymer* **1987**, *28*, 1772.
(10) Kricheldorf, H. R.; Pakull, R. *Macromolecules* **1988**, *21*, 551.
(11) Leland, M.; Zhang, A.-Q.; Ho, R.-M.; Cheng, S. Z. D.; Keller, A.; Kricheldorf, H. R. *Macromolecules* **1997**, *30*, 5249.
(12) Krigbaum, W. R.; Ciferri, A.; Acierno, D. *J. Appl. Polym. Sci., Appl. Polym. Symp.* **1985**, *41*, 293.
(13) Krigbaum, W. R.; Watanabe, J. *Polymer* **1983**, *24*, 1299.
(14) Romo-Uribe, A.; Windle, A. H. *Macromolecules* **1996**, *29*, 6246.
(15) Tokita, M.; Takahashi. T.; Hayashi, M.; Inomata, K.; Watanabe, J. *Macromolecules* **1996**, *29*, 1345.
(16) Cheng, S. Z. D.; Yoon, Y.; Zhang, A.-Q.; Savitski, E. P.; Park, J.-Y.; Percec, V.; Chu, P. *Macromol. Rapid Commun.* **1995**, *16*, 533.
(17) Yoon, Y; Zhang, A.; Ho, R.-M.; Cheng, S. Z. D.; Percec, V.; Chu, P. *Macromolecules* **1996**, *29*, 294.
(18) Yoon, Y.; Ho, R.-M.; Moon, B.; Kim, D.; McCreight, K. W.; Li, F.-M.; Harris, F. W.; Cheng, S. Z. D.; Percec, V.; Chu, P. *Macromolecules* **1996**, *29*, 3421.
(19) Gray, G. W.; Goodby, J. W. G. *Smectic Liquid Crystals*; Leonard Hill: London, 1984.
(20) Pershan, P. S. *Structure of Liquid Crystal Phases*; World Scientific: Teaneck, NJ, 1988.
(21) Chaikin, P. M.; Lubensky, T. C. *Principles of Condensed Matter Physics*; Cambridge: New York, 1995.
(22) Eashoo, M.; Wu, Z.; Zhang, A.; Shen, D.; Tse, C.; Harris, F. W.; Cheng, S. Z. D.; Gardner, K. H.; Hsiao, B. S. *Macromol. Chem. Phys.* **1994**, *195*, 2207.
(23) Kricheldorf, H. R.; Linzer, V.; Leland, M.; Cheng, S. Z. D. *Macromolecules* **1997**, *30*, 4828.

MA971198J